Giant resonances in ^{112}Sn and ^{124}Sn: Isotopic dependence of monopole resonance energies

Y.-W. Lui, D. H. Youngblood, Y. Tokimoto, H. L. Clark, and B. John*
Cyclotron Institute, Texas A&M University, College Station, Texas 77843, USA
(Received 6 April 2004; published 14 July 2004)

The giant resonance region from 10 MeV$<E_x<$55 MeV in ^{112}Sn and ^{124}Sn has been studied with inelastic scattering of 240 MeV α particles at small angles including 0°. Essentially, all of the expected isoscalar $E0-E3$ strength was located in both nuclei. The isotopic dependence of the giant monopole resonance energies was found to be consistent with relativistic and nonrelativistic calculations for interactions with $K_{\mathrm{NM}}\sim 220-240$ MeV.

DOI: 10.1103/PhysRevC.70.014307 PACS number(s): 25.55.Ci, 24.30.Cz, 27.60.+j

I. INTRODUCTION

The locations of the isoscalar giant monopole (GMR) and giant dipole (ISGDR) resonances are important because their energies can be directly related to the nuclear compressibility, and from this, the compressibility of nuclear matter (K_{NM}) can be obtained [1,2]. Of particular interest is the variation of compressibility with neutron number. We recently reported measurements for ^{110}Cd and ^{116}Cd [3], where the energy difference between the $E0$ positions was consistent with relativistic calculations and with calculations using modified Skyrme interactions (differing from Skyrme primarily in the behavior of the density dependence to provide a more reliable extrapolation to neutron rich systems), but not with those using more conventional Skyrme interactions. A much larger isotopic range (12 instead of 6) can be obtained by studying ^{112}Sn and ^{124}Sn. Studies of the GMR in the Sn isotopes were carried out a number of years ago [4,5], but this early data has relatively large errors compared to what is now possible. Furthermore, because of the much improved peak-to-continuum ratio [6] we can now look at the actual distribution of strength, as well as the behavior of the ISGDR, which was not possible then. With this in mind, we have studied ^{112}Sn and ^{124}Sn with small-angle inelastic α scattering at 240 MeV, which has been very useful in obtaining strength distributions of isoscalar electric multipoles in several nuclei [6].

II. EXPERIMENTAL TECHNIQUE AND DATA ANALYSIS

The experimental technique has been described thoroughly in Ref. [6] and is summarized briefly below. Beams of 240 MeV α particles from the Texas A&M K500 superconducting cyclotron bombarded self-supporting Sn foils of 5.8 mg/cm^2 (^{112}Sn) and 12.8 mg/cm^2 (^{124}Sn) thickness, enriched to more than 96% in the desired isotope, and located in the target chamber of the multipole-dipole-multipole spectrometer. The horizontal acceptance of the spectrometer was 4° and ray tracing was used to reconstruct the scattering angle. The vertical acceptance was set at ±2°. The focal plane detector measured the position and angle in the scattering plane and covered from $E_x\sim 8$ MeV to $E_x\sim 55$ MeV, depending on the scattering angle. The out-of-plane scattering angle was not measured. A position resolution of approximately 0.9 mm and a scattering angle resolution of about 0.09° were obtained. At $\theta_{\mathrm{spec}}=0°$, runs with an empty target frame had an α-particle rate approximately 1/2000 of that with a target in place, and α particles were uniformly distributed in the spectrum. Cross sections were obtained from the charge collected, target thickness, dead time, and known solid angle. The target thicknesses were measured by weighing and checked by measuring the energy

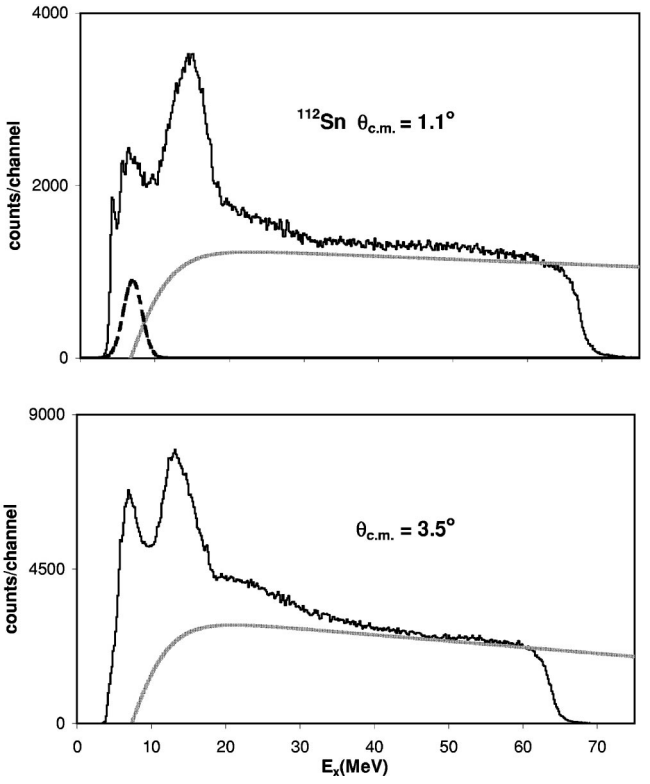

FIG. 1. Inelastic α spectra obtained at two angles for ^{112}Sn. The thick gray lines show the continuum chosen for the analysis. The dashed line below 10 MeV represents a contaminant peak present at some angles in the spectra taken with the spectrometer at 0°. This was subtracted before the multipole analysis was done.

*Present address: Nuclear Physics Division, Bhabha Atomic Research Center, Mumbai-400085, India.

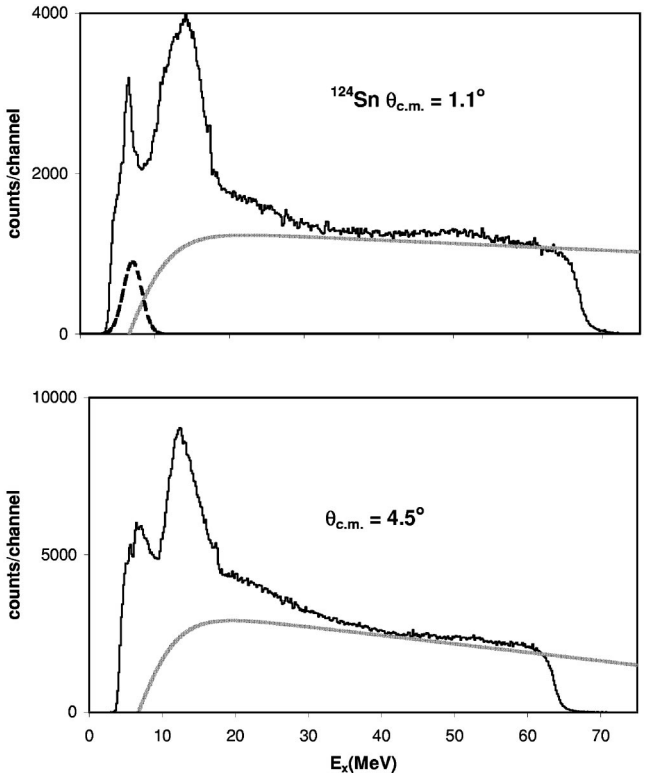

FIG. 2. Inelastic α spectra obtained at two angles for ^{124}Sn. See caption of Fig. 1 for explanation.

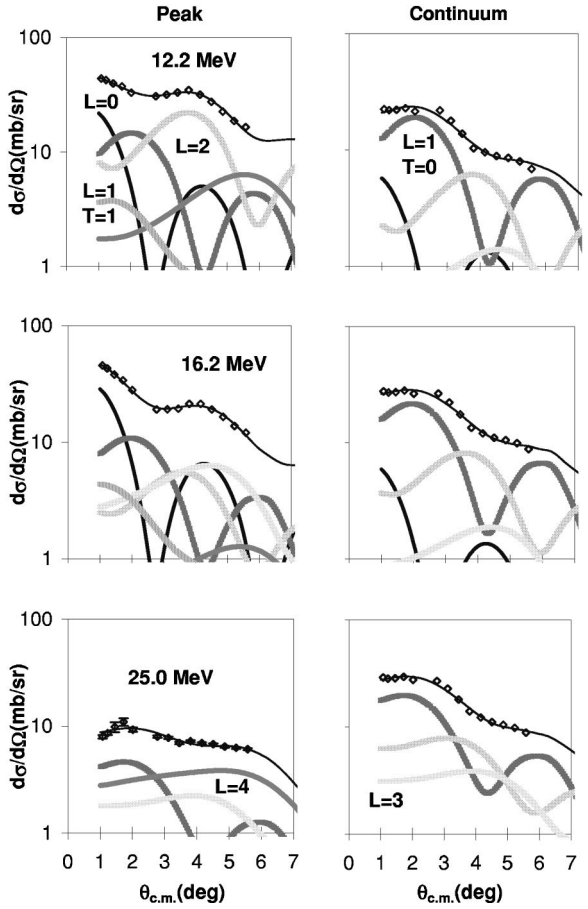

FIG. 3. The angular distributions of the ^{112}Sn cross sections for an 800-keV-wide bin centered at the excitation energy indicated on the figure (in MeV) for inelastic α scattering for three excitation ranges of the GR peak and the continuum. The lines through the data points indicate the multipole fits. Contributions of each multipole are shown. The statistical errors are smaller than the data points.

loss of the 240 MeV α beam in each target. The cumulative uncertainties in target thickness, solid angle, etc., result in about a ±10% uncertainty in absolute cross sections. ^{24}Mg spectra were taken before and after each run with each target, and the 13.85±.02 MeV $L=0$ state [7] was used as a check on the calibration in the giant resonance region.

Sample spectra obtained for ^{112}Sn are shown in Fig. 1, and for ^{124}Sn in Fig. 2. The giant resonance peak can be seen extending up past $E_x=30$ MeV. The spectrum was divided into a peak and a continuum, where the continuum was assumed to have the shape of a straight line at high excitation, joining onto a Fermi shape at low excitation to model particle threshold effects [6]. Samples of the continua used are shown in the figures.

III. MULTIPOLE ANALYSIS

The multipole components of the giant resonance peak were obtained [6] by dividing the peak into multiple regions (bins) by excitation energy and then comparing the angular distributions obtained for each of these bins to distorted-wave Born approximation (DWBA) calculations. The uncertainty from the multipole fits was determined for each multipole by incrementing (or decrementing) that strength, then adjusting the strengths of the other multipoles to minimize total χ^2. This continued until the new χ^2 was one unit larger than the total χ^2 obtained for the best fit.

Elastic-scattering data were not available for ^{112}Sn or ^{124}Sn, so optical model parameters obtained for ^{116}Sn [8] were used. Single-folding density-dependent DWBA calculations (as described in Refs. [6,8,9]) were carried out with Fermi mass distributions for ^{112}Sn and ^{124}Sn using $c=5.3714$ and 5.4907 fm, respectively, and $a=0.523$ fm for both nuclei [10]. The transition densities, sum rules, and DWBA calculations were discussed thoroughly in Ref. [6] and, except for the isoscalar dipole, the same expressions and techniques were used in this work. The transition density for inelastic-α-particle excitation of the ISGDR given by Harakeh and Dieperink [11] (and described in Ref. [6]) is for only one magnetic substate, so that the transition density given in Ref. [11] must be multiplied by the square root of 3 in the DWBA calculation.

A sample of the angular distributions obtained for the giant resonance (GR) peak and the continuum are shown for ^{112}Sn in Fig. 3 and ^{124}Sn in Fig. 4. Fits to the angular distributions were carried out with a sum of isoscalar 0^+, 1^-, 2^+, 3^-, and 4^+ strengths. The isovector giant dipole resonance (IVGDR) contributions were calculated from the known distributions [12] for ^{124}Sn and held fixed in the fits. The ^{116}Sn IVGDR distribution, shifted in energy by $1/A^{1/3}$, was used for ^{112}Sn. Sample fits obtained, along with the individual

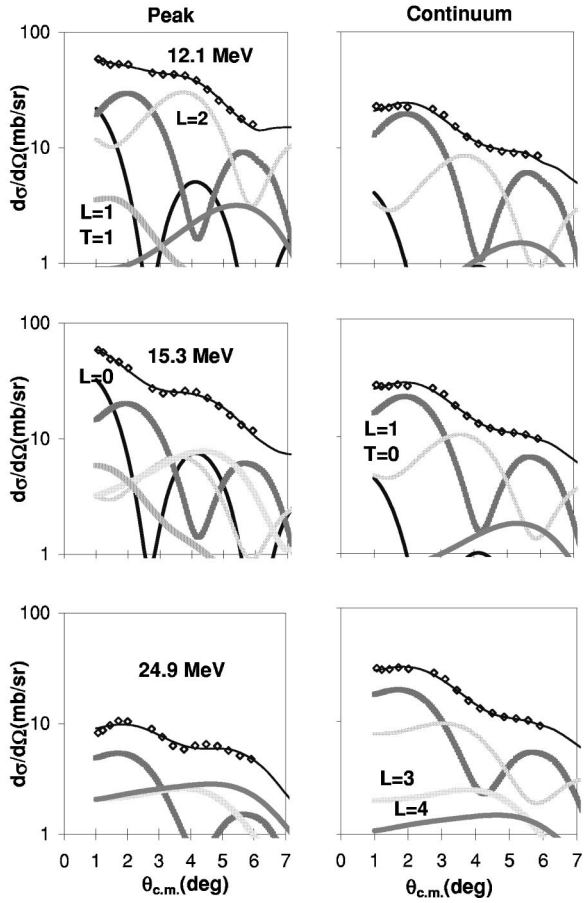

FIG. 4. The angular distributions of the ^{124}Sn cross sections for an 800-keV-wide bin centered at the excitation energy indicated on the figure (in MeV) for inelastic α scattering for three excitation ranges of the GR peak and the continuum. The lines through the data points indicate the multipole fits. Contributions of each multipole are shown. The statistical errors are smaller than the data points.

components of the fits, are shown superimposed on the data in Figs. 3 and 4. The continuum distributions are similar over the entire energy range, whereas the angular distributions of the cross sections for the peak change as the contributions of different multipoles dominate in different energy regions.

Several analyses were carried out to assess the effects of different choices of the continuum on the resulting multipole distributions, as described in Ref. [13] where the continuum was systematically varied and the data reanalyzed. The strength distributions obtained from these analyses and from those obtained with the continua shown in the figures were then averaged, and errors calculated by adding the errors obtained from the multipole fits in quadrature to the standard deviations between the different fits. The (isoscalar) $E0$, $E1$, and $E2$ and $E3$ multipole distributions obtained are shown in Figs. 5 and 6, and the energy moments and sum-rule strengths obtained are summarized in Tables I and II. Due to the limited angular range of the data, $E4$ strength could not be distinguished from higher multipoles and those results are not included. Single Gaussians were also fit to the $E0$ and $E2$ distributions and two Gaussians were fit to the $E1$ distributions. These are shown in Figs. 5 and 6 and the parameters obtained are listed in Tables I and II.

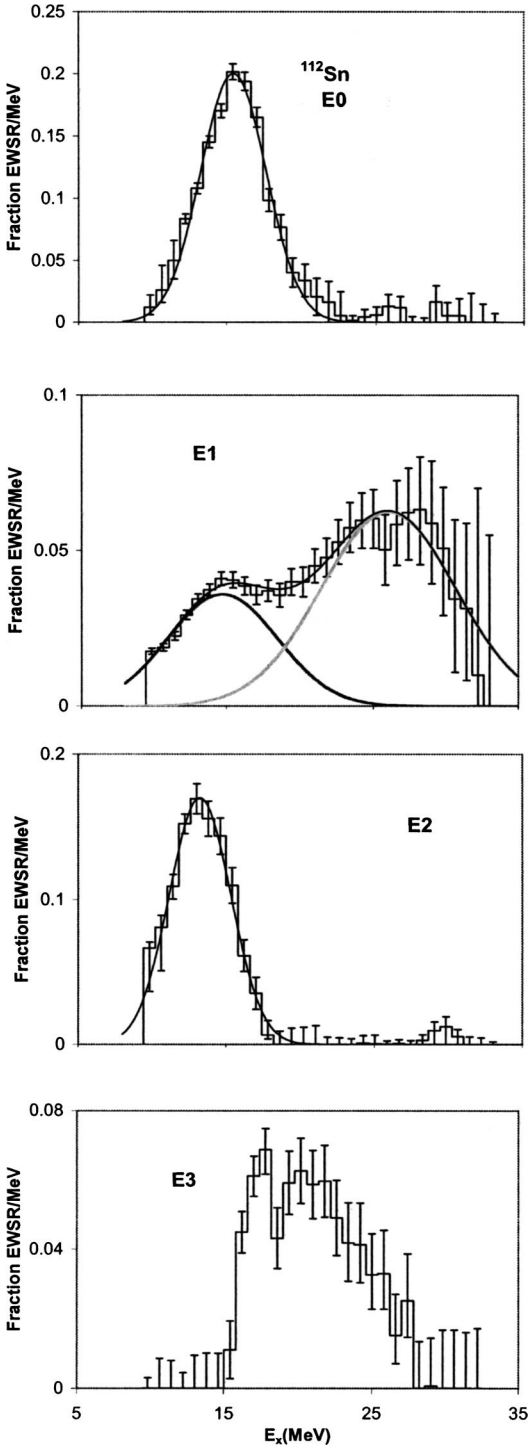

FIG. 5. Strength distributions obtained for ^{112}Sn are shown by the histograms. Error bars represent the uncertainty due to the fitting of the angular distributions and different choices of the continuum, as described in the text. The smooth lines show Gaussian fits.

IV. DISCUSSION

In both nuclei, strength consistent with 100% of the energy-weighted sum rule (EWSR) was located in a rela-

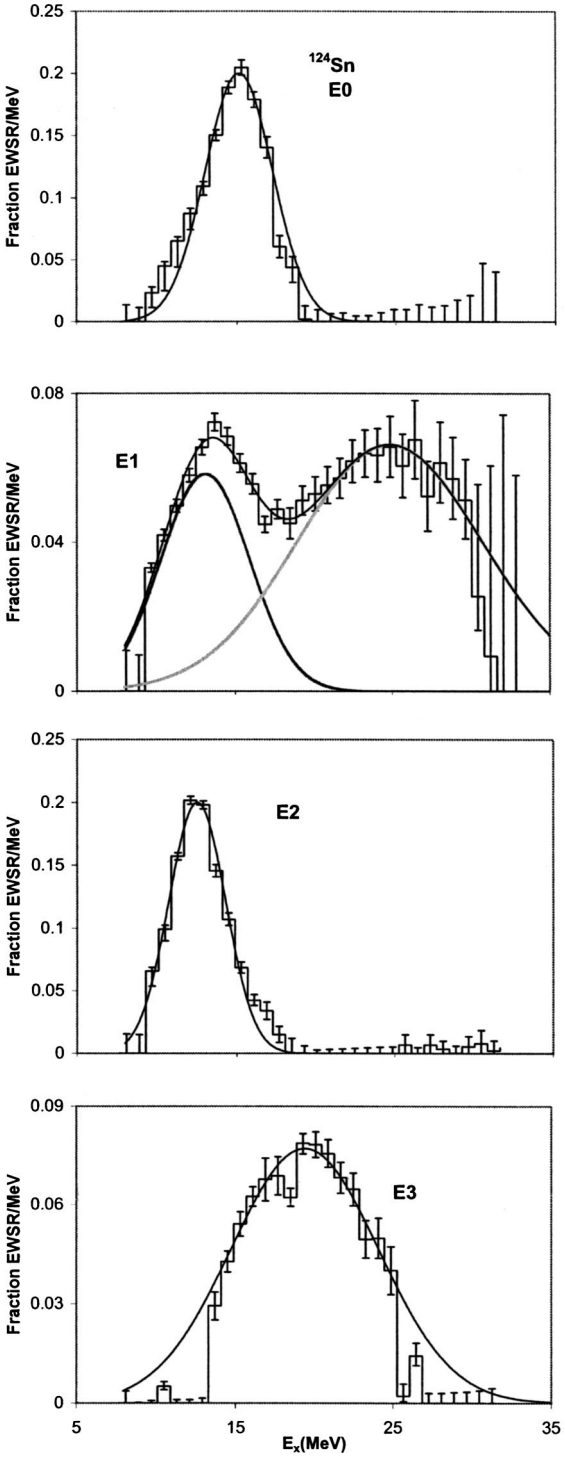

FIG. 6. Strength distributions obtained for ^{124}Sn are shown by the histograms. Error bars represent the uncertainty due to the fitting of the angular distributions and different choices of the continuum, as described in the text. The smooth lines show Gaussian fits.

tively narrow peak for both $E0$ and $E2$ transitions, with the $E2$ strength in both nuclei and the $E0$ strength in ^{112}Sn having an almost Gaussian shape. The $E0$ strength in ^{124}Sn has significant tailing on the low-energy side, shifting energy moments lower relative to the peak position. The uncertainties in the region around $E_x = 10$ MeV are larger than at higher excitation due to a rapidly varying solid angle near the low-energy cutoff in the detector, and the uncertainty caused by the presence or some real background in this region (seen as a dashed peak in Figs. 1 and 2). Previous measurements of $E0$ and $E2$ GR strength in ^{112}Sn and ^{124}Sn were reported by Youngblood *et al.* and Lui *et al.* [5], as well as Sharma *et al.* [4], using inelastic α scattering, and their results are also summarized in Tables I and II. Their analyses assumed the peaks were Gaussian in shape. The Gaussian centroids we obtained agree within the errors with those obtained previously for both the $E0$ and $E2$ distributions, though the widths we obtain are somewhat larger.

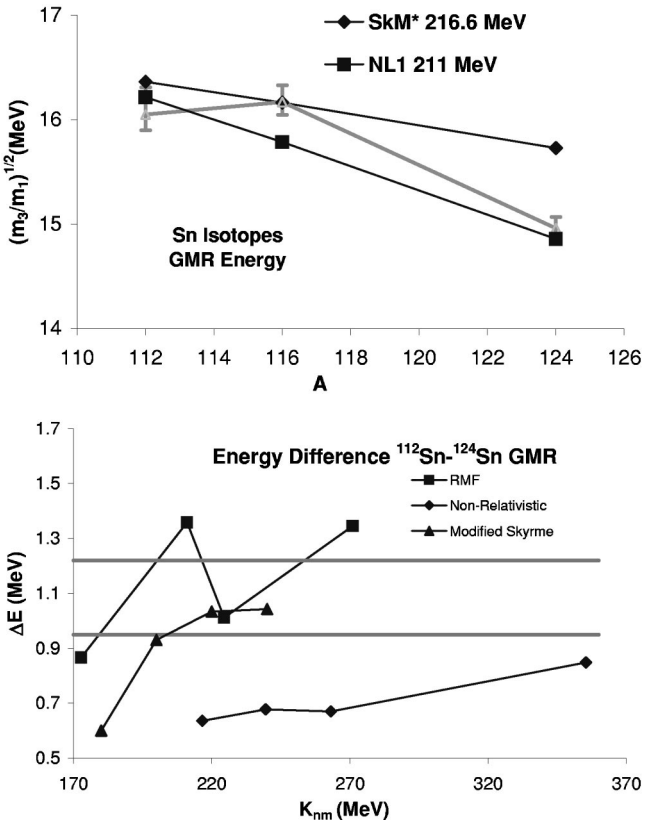

FIG. 7. (Top) GMR energies calculated with the relativistic mean-field parametrization [20] and nonrelativistic parametrizations [18] are compared to the experimental energies shown in gray. The error bars include systematic errors. (Bottom) The difference in GMR energies $[(m_3/m_1)^{1/2}]$ between ^{112}Sn and ^{124}Sn calculated with the relativistic mean-field parametrization [20], nonrelativistic parametrizations [18], and modified Skyrme [19] are compared to the experimental difference whose limits are indicated by the horizontal gray lines. The experimental range shown includes statistical errors, but not systematic errors.

There have been no previous reports of isoscalar dipole or $3\hbar\omega$ $E3$ strength in ^{112}Sn or ^{124}Sn. The isoscalar dipole resonance is known to consist of two components [14–16] and this is seen clearly in Figs. 3 and 4. In both nuclei, $E1$ strength consistent with 100% of the ISGDR EWSR was identified with approximately one-third of the strength in the lower component. $E3$ strength in nuclei is split into $1\hbar\omega$ and $3\hbar\omega$ components [17], but little if any of the $1\hbar\omega$ strength

TABLE I. Parameters obtained for isoscalar multipoles in ^{112}Sn.

	Moments											
	$E0$	− error	+ error	$E1$	− error	+ error	$E2$	− error	+ error	$E3$	− error	+ error
m_1 (Frac EWSR)	1.16	0.18	0.13	0.96	0.11	0.11	0.87	0.10	0.10	0.57	0.06	0.08
m_1/m_0 (MeV)	15.43	0.10	0.11	20.33	0.28	0.28	13.23	0.14	0.18	20.63	0.28	0.30
rms width (MeV)	2.57	0.19	0.46	6.18	0.32	0.34	1.91	0.09	0.77	3.21	0.10	0.46
$(m_3/m_1)^{1/2}$ (MeV)	16.05	0.14	0.26									
$(m_1/m_{-1})^{1/2}$ (MeV)	15.23	0.10	0.10									

	Gaussian fits											
	$E0$	− error	+ error	$E1$ Pk1	− error	+ error	$E1$ Pk2	− error	+ error	$E2$	− error	+ error
Centroid (MeV)	15.67	0.11	0.11	14.92	0.14	0.15	26.28	0.23	0.32	13.48	0.14	0.15
FWHM (MeV)	5.18	0.04	0.40	8.82	0.29	0.26	10.82	0.36	0.39	4.90	0.27	0.22
Fraction EWSR	1.10	0.12	0.15	0.32	0.04	0.04	0.70	0.10	0.10	0.88	0.13	0.14

	Sharma *et al.* [4]		Lui *et al.* [5]	
	$E0$	$E2$	$E0$	$E2$
Centroid (MeV)	15.88±0.14	13.51±0.13	15.7±0.3	13.3±0.2
FWHM (MeV)	3.30±0.25	3.15±0.23	4.2±0.3	3.5±0.2
Fraction EWSR	1.06±0.24	1.23±0.26	1.66±0.60	0.57±0.20

was seen. Around 75% of the $E3$ strength should be in the $3\hbar\omega$ component, and this is consistent with the $E3$ strength observed in ^{124}Sn, though only ~57% was identified in ^{112}Sn.

There are no specific calculations for $E0$ strength in ^{112}Sn or ^{124}Sn, however Nayak *et al.* [18] have carried out Hartree-Fock random-phase approximation (RPA) calculations with several Skyrme or Skyrme-like interactions and parametrized the results in terms of the Leptodermous expansion. Farine *et al.* [19] carried out a study using modified Skyrme interactions (parametrized with the Leptodermous expansion) designed to explore how the effective $K_{\rm NM}$ for an interaction might be changed, while still providing breathing mode energies consistent with experimental results. Chossy and Stocker [20] have carried out a similar parametrization for several relativistic parameter sets. $E0$ energies calculated with relativistic and nonrelativistic interactions are compared to the experimental energies $[(m_3/m_1)^{1/2}]$ for the Sn isotopes in the top panel of Fig. 7. The ^{116}Sn result shown was obtained from data taken along with the data for ^{112}Sn and ^{124}Sn, and is in excellent agreement with that reported in Refs. [13,21], obtained in different experimental runs. The GMR energies in ^{112}Sn and ^{124}Sn appear to be low compared to ^{116}Sn. Previously it was found that the GMR in ^{116}Cd was also lower than expected relative to ^{116}Sn [3]. The experimental energies for ^{112}Sn and ^{124}Sn are slightly below energies obtained with calculations for interactions for which $K_{\rm NM}$~211–216 MeV. This is somewhat lower than $K_{\rm NM}$ ~231 MeV, suggested by energies for a number of other nuclei [20] including ^{116}Sn.

The energy difference between the ^{112}Sn and ^{124}Sn is much better determined than the actual energy, as systematic errors (such as strength errors at around 10 MeV due to background, detector threshold effects, continuum choices) should be similar for both nuclei. This difference might be expected to depend mostly on the symmetry term [dependent on $(N\text{-}Z)/A$] in the Leptodermous expansion, and that is the largest contribution. The lower panel in Fig. 7 compares calculations for the energy difference between the GMR's in ^{112}Sn and ^{124}Sn using the parametrizations of Nayak *et al.*, Chossy and Stocker, and Farine *et al.*, with the experimental difference. Except for the $S3$ interaction ($K_{\rm NM}$=333 MeV), each of the nonrelativistic interactions used by Nayak *et al.* results in an energy difference much lower than the experimental results. Of the energy differences calculated with the relativistic interactions, only that for NL-C ($K_{\rm NM}$ =224.6 MeV) falls in the experimental range. The results from the modified Skyrme interactions with $K_{\rm NM}$=220 and

TABLE II. Parameters obtained for isoscalar multipoles in ^{124}Sn.

	Moments											
	$E0$	− error	+ error	$E1$	− error	+ error	$E2$	− error	+ error	$E3$	− error	+ error
m_1 (Frac EWSR)	1.04	0.11	0.11	1.20	0.17	0.15	0.91	0.10	0.10	0.73	0.08	0.08
m_1/m_0 (MeV)	14.50	0.14	0.14	18.46	0.22	0.42	12.81	0.10	0.14	19.12	0.26	0.26
rms width (MeV)	2.09	0.09	0.13	6.34	0.20	1.10	1.90	0.05	0.10	3.30	0.05	0.17
$(m_3/m_1)^{1/2}$ (MeV)	14.96	0.11	0.10									
$(m_1/m_{-1})^{1/2}$ (MeV)	14.33	0.14	0.17									

	Gaussian fits											
	$E0$	− error	+ error	$E1$ Pk1	− error	+ error	$E1$ Pk2	− error	+ error	$E2$	− error	+ error
Centroid (MeV)	15.34	0.13	0.13	13.31	0.15	0.15	25.06	0.21	0.22	12.72	0.11	0.11
FWHM (MeV)	5.00	0.53	0.03	6.60	0.13	0.15	13.87	0.28	0.24	4.20	0.03	0.32
Fraction EWSR	1.06	0.20	0.10	0.40	0.04	0.04	0.93	0.13	0.12	0.89	0.10	0.15

	Sharma *et al.* [4]		Youngblood *et al.* [5]	
	$E0$	$E2$	$E0$	$E2$
Centroid (MeV)	15.35±0.16	13.02±0.13	14.8±0.4	12.3±0.4
FWHM (MeV)	3.40±0.35	2.80±0.30	3.8±0.6	3.1±0.3
Fraction EWSR	1.08±0.22	1.27±0.31	1.86±0.60	0.78±0.25

240 MeV are consistent with the data, while that for SkK200 is just outside the experimental range. These results are consistent with a similar comparison done for ^{110}Cd and ^{116}Cd [3].

V. CONCLUSIONS

Most of the expected isoscalar $E0-E3$ strength in ^{112}Sn and ^{124}Sn has been identified. Predictions using relativistic and nonrelativistic (Skyrme or Skyrme-like) interactions with $K_{\mathrm{NM}}\sim 211-216$ MeV result in energies consistent with the experimental energies. The more accurate energy difference between the $E0$ positions in ^{112}Sn and ^{124}Sn is consistent with relativistic calculations for the NL-C parametrization ($K_{\mathrm{NM}}=224.5$ MeV) and with calculations using modified Skyrme interactions having $K_{\mathrm{NM}}=220$ and 240 MeV, differing from Skyrme primarily in the behavior of the density dependence to provide a more reliable extrapolation to neutron-rich systems. The GMR energies in ^{112}Sn and ^{124}Sn are lower than would be expected from extrapolations based on the ^{116}Sn GMR energy, particularly for ^{112}Sn, where $1/A^{1/3}$ dependence alone should result in a GMR energy higher than for ^{116}Sn, in contrast with the experimental result, where the GMR energies in ^{112}Sn and ^{116}Sn are the same.

ACKNOWLEDGMENTS

This work was supported in part by the U.S. Department of Energy under Grant No. DE-FG03-93ER40773 and by The Robert A. Welch Foundation.

[1] J. P. Blaizot, Phys. Rep. **64**, 171 (1980).
[2] S. Stringari, Phys. Lett. **108**, 232 (1982).
[3] Y.-W. Lui, D. H. Youngblood, Y. Tokimoto, H. L. Clark, and B. John, Phys. Rev. C **69**, 034611 (2004).
[4] M. M. Sharma, W. T. A. Borghols, S. Brandenburg, S. Crona, A. Van der Woude, and M. N. Harakeh, Phys. Rev. C **38**, 2562 (1988).
[5] D. H. Youngblood, P. Bogucki, J. D. Bronson, U. Garg, Y.-W. Lui, and C. M. Rozsa, Phys. Rev. C **23**, 1997 (1981); Y.-W. Lui, P. Bogucki, J. D. Bronson, D. H. Youngblood, and U. Garg, *ibid.* **30**, 51 (1984).
[6] D. H. Youngblood, Y.-W. Lui, and H. L. Clark, Phys. Rev. C **65**, 034302 (2002); **63**, 067301 (2001); **60**, 014304 (1999).
[7] K. van der Borg, M. N. Harakeh, and A. van der Woude, Nucl. Phys. **A365**, 243 (1981).
[8] H. L. Clark, Y.-W. Lui, and D. H. Youngblood, Phys. Rev. C **57**, 2887 (1998).
[9] G. R. Satchler and D. T. Khoa, Phys. Rev. C **55**, 285 (1997).
[10] G. Fricke, C. Bernhardt, K. Heilig, L. A. Schaller, L. Schellenberg, E. B. Shera, and C. W. DeJager, At. Data Nucl. Data Tables **60**, 177 (1995).
[11] M. N. Harakeh and A. E. L. Dieperink, Phys. Rev. C **23**, 2329 (1981).
[12] S. S. Dietrich and B. L. Berman, At. Data Nucl. Data Tables **38**, 199 (1988).
[13] D. H. Youngblood, Y.-W. Lui, H. L. Clark, B. John, Y. Tokimoto, and X. Chen, Phys. Rev. C **69**, 034315 (2004).
[14] H. L. Clark, Y.-W. Lui, and D. H. Youngblood, Phys. Rev. C **63**, 031301 (2001).
[15] G. Colo, N. Van Giai, P. F. Bortignon, and M. R. Quaglia, Phys. Lett. B **485**, 362 (2000).
[16] D. Vretenar, A. Wandelt, and P. Ring, Phys. Lett. B **487**, 334 (2000).
[17] J. M. Moss, D. H. Youngblood, C. M. Rozsa, D. R. Brown, and J. D. Bronson, Phys. Rev. Lett. **37**, 816 (1976).
[18] R. C. Nayak, J. M. Pearson, M. Farine, P. Gleissl, and M. Brack, Nucl. Phys. **A516**, 62 (1990).
[19] M. Farine, J. M. Pearson, and F. Tondeur, Nucl. Phys. **A615**, 137 (1997).
[20] T. V. Chossy and W. Stocker, Phys. Rev. C **56**, 2518 (1997).
[21] D. H. Youngblood, H. L. Clark, and Y.-W. Lui, Phys. Rev. Lett. **82**, 691 (1999).